10th International Conference on Fracture Mechanics of Concrete and Concrete Structures
FraMCoS-X
G. Pijaudier-Cabot, P. Grassl and C. La Borderie (Eds)
https://doi.org/10.21012/FC10.235158

CREATING STRAIN HARDENING CEMENTITIOUS COMPOSITES (SHCCS) THROUGH USE OF ADDITIVELY MANUFACTURED POLYMERIC MESHES AS REINFORCEMENT

YADING XU, ERIK SCHLANGEN AND BRANKO ŠAVIJA

Faculty of Civil Engineering and Geosciences, Delft University of Technology
Stevinweg 1, 2628CN, Delft, Netherlands
e-mail: {y.xu-5; erik.shclangen; b.savija}@tudelft.nl

Key words: Cohesive fracture, Fiber Reinforced Concrete, Composites, Durability

Abstract: Strain hardening cementitious composites are a class of cementitious materials showing metal-like (i.e. pseudo-plastic) behavior in tension due to their multiple cracking ability. This is commonly achieved through use of fiber reinforcement (such as PVA) or, similarly, textile reinforcement (TRC). Increasing the ductility is important in applications such as e.g. earthquake zones, where this enables absorption of large amounts of energy. On the other hand, tight cracks are important for ensuring the protection of the reinforcing steel and hence the durability of a reinforced concrete structure. This research presents an alternative approach – creating strain hardening cementitious composites by using additively manufactured (3D printed) polymeric meshes instead of fiber or textile reinforcement. Different designs of polymeric meshes were manufactured and cast in mortar. They were subsequently tested in four-point bending and uniaxial tension. The results show that properly designed polymeric meshes enabled deflection hardening or strain hardening to be achieved, either through slip hardening of the polymeric reinforcement or through multiple microcracking. Furthermore, it was possible to create a simple functionally graded cementitious composite, in which denser reinforcement was used in the constant moment region of the 4-point bending specimen compared to the outer regions, without loss of ductility. This study shows great potential of 3D printing for customization of cementitious composites.

1 INTRODUCTION

Concrete is a versatile construction material with excellent properties. It is cheap, durable, and widely available. Concrete is, however, susceptible to cracking: although it has good compressive strength, it is relatively weak in tension. The brittleness of concrete can be overcome to a certain extent through use of fibres, such as steel or glass fibres [1]. A new class of ultraductile cementitious composites – strain hardening cementitious composites (SHCCs) – has been under development since the 90's. SHCCs are able to achieve very high strain capacity (several %) through controlled tightly spaced microcracking of the matrix [2]. This is achieved through micromechanical design and a small amount of PVA fibres (2%). However, in practical applications, problems arise with fibre agglomeration and preferential orientation of fibres following concrete flow during casting. If textile reinforcement is used (in textile reinforced concrete – TRC), such problems can be avoided.

In the past few years, a viable alternative to textile reinforcement has emerged. Additive manufacturing (commonly referred to as 3D printing) enables creation of polymeric micro-reinforcement with complex shapes. In recent years, several publications have been devoted

to this: Nam et al. [3] created random polymeric networks for replacing fibre reinforcement with fused deposition modelling (FDM) technique; Rosewitz et al. [4] used FDM to create biomimetic architectures to reinforce brittle mortar and enhance its mechanical response. It is clear that 3D printing offers numerous possibilities for replacing conventional fibre reinforcement.

Herein, we present the development of cementitious composites reinforced with 3D printed polymeric meshes [5]. Different geometries were fabricated and tested. Ideally, these composites should have strain hardening behaviour.

2 EXPERIMENTAL

2.1 Materials

Specimens with a cementitious matrix were reinforced with 3D printed polymeric meshes. For the matrix material, the mix used 550 kg/m^3 of Portland cement (CEM I 42.5N), 650 kg/m^3 of fly ash, 550 kg/m^3 of sand (0.125-0.25 mm), 2 kg/m^3 of superplasticizer (Glenium 51), and 395 kg/m^3 of water. The water/binder ratio of the material was set as 0.33.

Reinforcement meshes were manufactured with an FDM based 3D printer, Ultimaker 2+. In FDM, the model is printed layer by layer, by depositing the filament material from the bottom up. This can be a problem if long overhangs are printed, and could result in their low quality. In this initial study, therefore, relatively simple mesh designs are used to avoid issues with printing quality. For the printing material, an acrylonitrile butadiene styrene (ABS) was used as a filament. This material has good resistance to high pH, which makes it a good choice as reinforcement in cement-based materials. Since printing parameters and the printing direction have an influence on the mechanical properties of the mesh [6], printing was performed in the direction parallel to the normal stress and printing parameters were kept constant for all prints. The parameters are given in Table 1. The actual fabrication procedure in the 3D printer is shown in Figure 2.

Table 1: Printing parameters used in this work

Printing parameter	Configuration
Nozzle diameter (mm)	0.8
Temperature (°C)	260
Layer height (mm)	0.2
Line width (mm)	0.7
Infill density (%)	100
Infill pattern	Lines
Printing speed (mm/s)	40

2.2 Design of reinforcement meshes

Two different mesh designs were printed and tested. The designs are all based on triangular lattices.

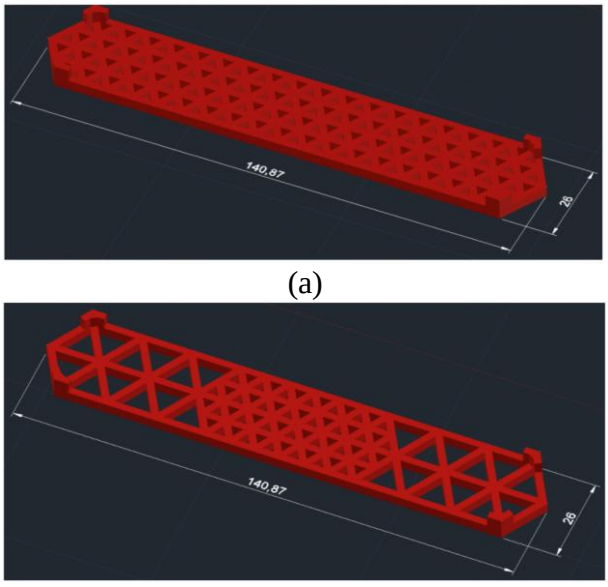

(a)

(b)

Figure 1: Design of reinforcement meshes in this study. (a) large triangles; (b) small triangles; (c) mixed triangles.

As shown in Figure 1, different sizes of triangles were used, as it was expected that the smaller triangles will provide a better reinforcement effect compared to larger triangles. This should, in principle, result in a better global behavior of the specimen. The second design uses larger triangles in the outer parts of the mesh, while the inner part has small triangles. This design was used only for the four-point bending test. The middle part of

the specimen is, in that case, subjected to a constant bending moment and is the area with the highest stresses, thereby needing more reinforcement. This design was an attempt of creating a simple functionally graded material, which "follow" the actual state of stress, something that cannot be done with traditional fiber or textile reinforcement.

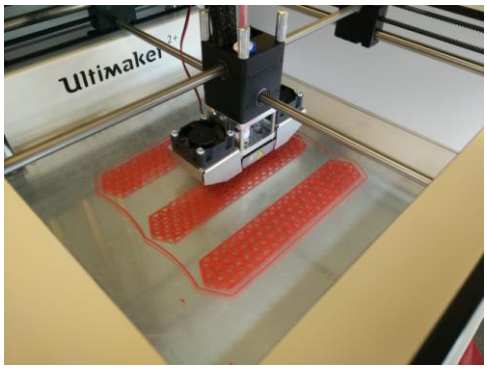

Figure 2: Fabrication of polymeric reinforcement using 3D printing.

2.3 Specimen preparation

Bottom surfaces of printed meshes were sanded for 30 seconds with sand paper prior to casting to remove the glue layer in contact with the build plate of the printer. Reinforcement meshes were placed in Styrofoam molds (190 x 180 x 8 mm) (Figure 3).

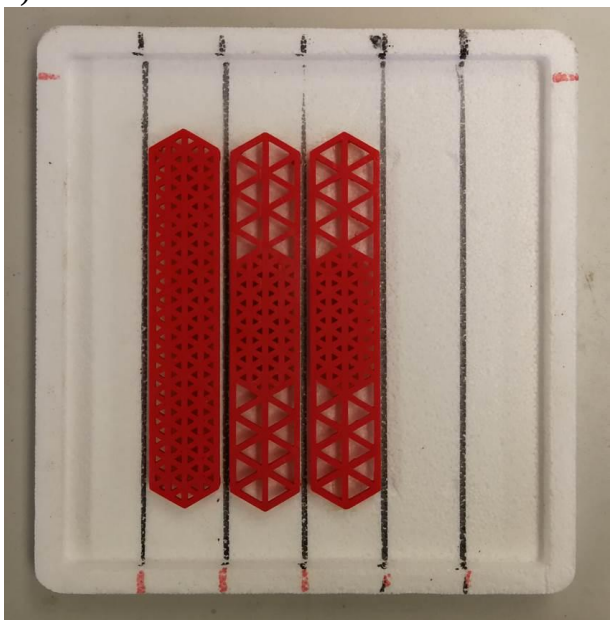

Figure 3: Reinforcement meshes placed in a styrofoam mold prior to casting.

The mixing of the mortar was as follows: first, solid ingredients were dry-mixed for four minutes in a laboratory mixed (Hobart). Afterwards, water and superplasticizer were added and the mixing continued for another four minutes. Subsequently, the fresh mix was poured into the prepared Styrofoam molds (with reinforcement meshes already in place) and vibrated for 30 seconds. The specimens were covered with plastics for 1 day (uniaxial tension) and 2 days (four-point bending), before demolding. Afterwards, they were cured in a fog room (20 ± 2°C, 96 ± 2%RH). One day before testing, the specimens were cut to appropriate size, as further described.

2.4 Four-point bending test

Testing was performed using an INSTRON 8872 testing apparatus under displacement control with a constant rate of 0.01 mm/s. The load was monitored with a load cell, while the deflection was measured by two LVDT's placed at the midspan. The specimen was 180 x 30 x 8mm, with a loading span of 120mm (Figure 4). In four-point bending, only small triangles and mix triangle designs were tested, in addition to reference specimens without reinforcement. For each series, 3 specimens were tested at 28 days.

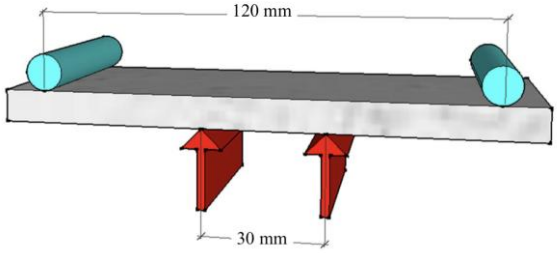

Figure 4: Four-point bending test setup

As previously described, the mixed triangle design was optimized for this loading setup, with the middle portion having a higher reinforcement ration provided by the smaller triangles. For each specimen, flexural strength and flexural deflection capacity were determined as shown in Figure 5.

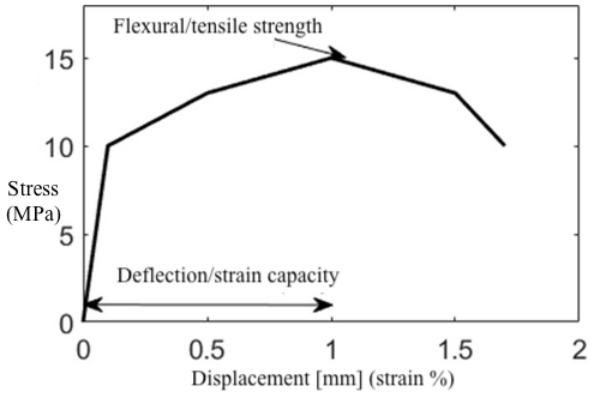

Figure 5: Definition of flexural/tensile strength and flexural deflection capacity/strain capacity as determined by four-point bending/uniaxial tensile tests (adapted from [7])

2.4 Uniaxial tensile testing

Uniaxial tensile tests were performed using an INSTRON 8872 apparatus under displacement control with a constant rate of 0.005 mm/s. The load was measured using a load cell, while the displacements were monitored using two LVDTs placed at the specimen sides. Before testing, specimens were glued on two parallel steel plates using a mix of PLEX 7742F glue and Pleximon. Specimen size for uniaxial tension testing was 10 x 30 x 8mm. During testing, images were taken using a digital camera. The images were then used to perform digital image correlation (DIC) analyses. The testing setup is shown in Figure 6. For uniaxial tension, 2 reference specimens and 4 small triangle specimens were tested.

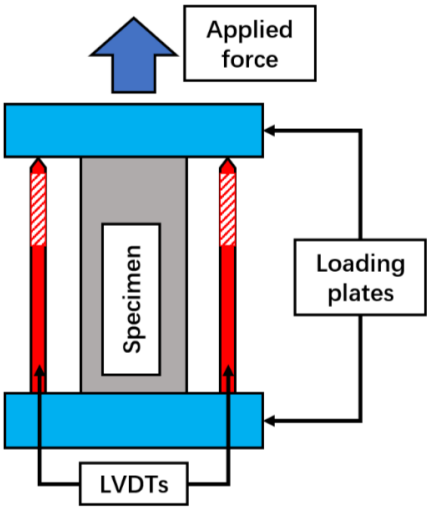

Figure 6: Schematic representation of the uniaxial tensile test.

3 RESULTS AND DISCUSSION

3.1 Four-point bending tests

Flexural stress/deflection curves (average deflection measured by the two LVDTs) for all specimens tested in four-point bending are given in Figure 7. A summary of the results is given in Table 2.

Table 2: A summary of four-point bending results (average values given only)

Series	First cracking strength (MPa)	Flexural strength (MPa)	Deflection capacity (mm)
Ref_{28}	4.99	4.99	0.343
ST_{28}	4.97	6.30	5.545
MT_{28}	5.26	6.16	4.985

As expected, the reference specimens show brittle behavior with a low deflection capacity. On the other hand, specimens reinforced with 3D printed meshes could undertake significantly higher deformation. For the small triangle design, all designs showed obvious deflection hardening behavior, whereby the loading that was reached after the first cracking was higher than the first cracking strength (see Figure 7b). This was clearly achieved through multiple microcracking, as in "regular" PVA fiber reinforced SHCC: each load drop in the stress/displacement curve signifies an occurrence of a crack. It is even more interesting to note that the mixed triangle series showed deflection hardening achieved through multiple microcracking (Figure 7c). This specimen series had significantly less reinforcement in terms of percentage due to the fact that a dense reinforcing mesh was used only in the middle portion of the sample, i.e. in the constant moment region exposed to the highest stresses. This simple modification shows great potential of additive manufacturing: it is possible to achieve significant savings in material costs if the reinforcement is designed and manufactured to cover only areas where it is needed (i.e. regions of high stress). Clearly, this is not possible when conventional fiber

reinforcement is used.

The results (Table 2) show that the addition of polymeric reinforcement meshes does not significantly influence the first cracking strength of the specimens. However, flexural strength is clearly increased by adding polymeric reinforcement by 26.2% and 23.4% for the small triangle and the mixed triangle design, respectively. This is clearly a result of deflection hardening in these specimens. The most important improvement is the increase in flexural deflection capacity: by 1516% and 1353% for the small triangle and the mixed triangle design, respectively. Therefore, it was possible to create graded cementitious composites and thereby optimizing material usage.

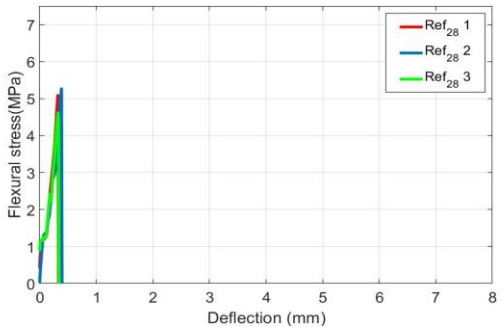

(a)

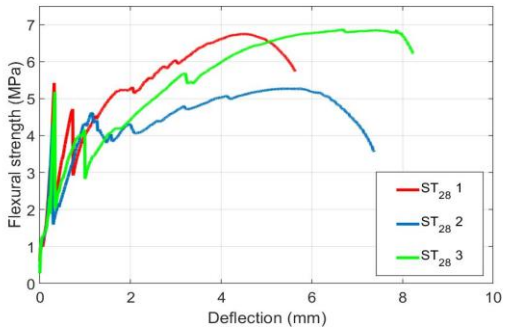

(b)

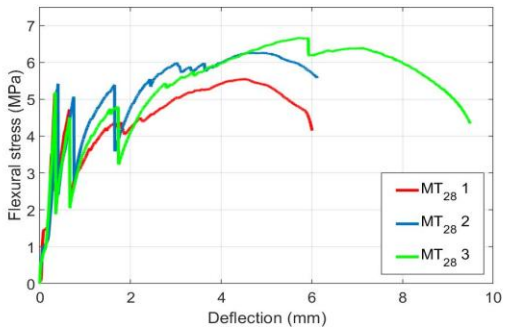

(c)

Figure 7: Flexural stress/deflection curves for specimens tested in four-point bending: (a) reference series; (b) small triangles; (c) mixed triangles.

3.2 Uniaxial tension tests

Results of uniaxial tensile testing are summarized in Table 3 and Figure 8. It is clear that the reference specimens (i.e. those not reinforced with 3D printed polymeric meshes) exhibit strain softening behavior typical of cementitious materials (Figure 8a). It has a low strain capacity and fails after a single crack localizes and opens. On the other hand, specimens reinforced with a 3D printed polymeric mesh (small triangle design) show clear strain hardening behavior (Figure 8b) and have a large strain capacity. This is a result of multiple microcracking (Figure 8c): the reinforcement is able to bridge the crack and keep it closed in order for other cracks to form. As also shown in Figure 8, increasing load was recorded in reinforced specimens after the first cracking formed. Again, each drop in the stress/strain curve indicates a formation of a new crack. The specimens finally fail through pullout of the polymeric reinforcement mesh and localization of a single wide crack. For the four tested specimens, the results are quite consistent and show little variation.

Table 3: Summary of the uniaxial tension results

Series	First cracking strength (MPa)	Tensile strength (MPa)	Strain capacity (mm)
Ref_{28}	3.44	3.44	0.021
ST_{28}	1.09	2.42	0.579

Compared to the reference specimens, reinforced specimens show a much lower first cracking strength. A reason for this is that the reinforcement might introduce numerous weak spots and/or air voids at the reinforcement/matrix interface, thereby providing numerous initiation points for the cracking. Furthermore, matrix compaction is more difficult in these specimens due to the spacing regions of the reinforcement, also possibly introducing imperfections. When it comes to tensile strength, in reinforced

specimens it is higher than the first cracking strength due to the strain hardening. The tensile strain capacity is significantly increased (more than 5000%).

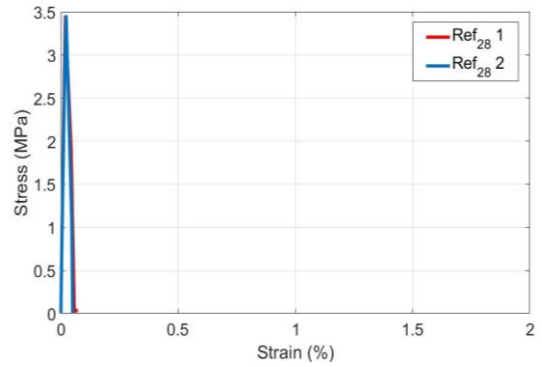

(a)

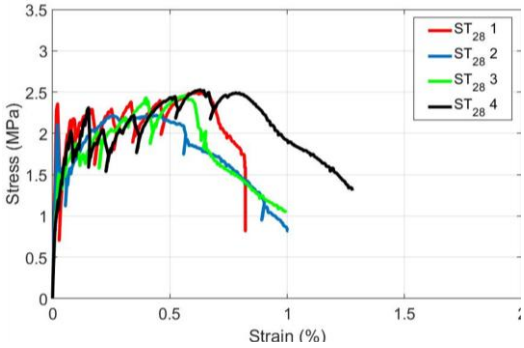

(b)

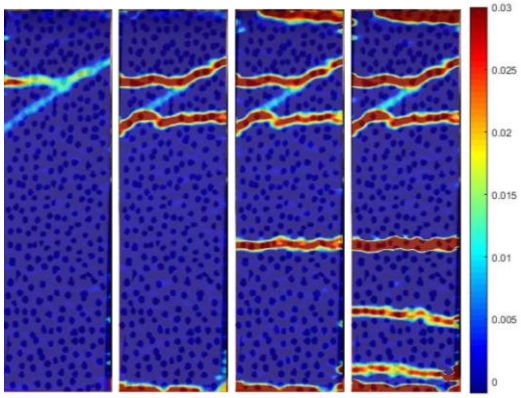

(c)

Figure 8: Tensile stress/strain curve for reference (a) and specimens reinforced with small triangles (b). In (c), results from DIC on a specimen with small triangle reinforcement are shown.

These results show that, even with simple reinforcement mesh designs used in this study, there are significant effects. Clearly, there is still room for improvement: more effort should be put in designing the polymeric reinforcement meshes. Furthermore, knowledge of the bond behavior between the mesh and the matrix needs to be acquired for appropriate micromechanical design. This indicates a huge potential that additive manufacturing has in creating strain hardening cementitious composites.

4 CONCLUSIONS

In this work, a preliminary study of using additively manufactured polymeric meshes as reinforcement for creating strain hardening cementitious composites. Simple reinforcement meshes were designed, manufactured, and tested in four-point bending and uniaxial tension. Based on the performed experiments, the following conclusions can be drawn:

- 3D printed polymeric meshes enable creating composites with strain hardening and deflection hardening behavior. This mainly depends on the mesh design in terms of a same matrix.
- The use of 3D printed polymeric reinforcement enables significantly increasing the deflection and tensile strain capacity of cementitious composites compared to the reference material.
- In four-point bending, a simple mesh design (MT) showed great potential of using additive manufacturing for creating functionally graded cementitious composites.

Although this research shows great potential of the proposed approach, there are still many issues that need to be studied. First, in this research, the focus was on the mesh design, while the cementitious matrix was kept constant. It should be noted, however, that the behavior of the composite does not depend only on the design of the reinforcement, but also on the matrix properties [8] [40]. In this research, a matrix with rather low w/b ratio (0.33) was used, resulting in a relatively strong material after 28 days, even higher deflection and strain capacity could be obtained with lower w/b ratio. Furthermore, no detailed knowledge of the bond behavior between the 3D printed polymeric reinforcement and the cementitious matrix is available. This will be a

part of future research. Finally, printing parameters of 3D printing were kept constant in this research. These parameters may significantly influence the properties of the printed reinforcement. This also needs to be investigated further in the future.

5. ACKNOWLEDGEMENTS

Yading Xu would like to acknowledge the funding supported by China Scholarship Council (CSC). under the grant CSC No.201708110187. The authors would like to acknowledge Mr. Vincent Huigen, Mr. Jorgi Penners and Mr. Bas Berger for their help in the sample preparing and mechanical tests.

REFERENCES

[1] Zollo, R.F., 1997. Fiber-reinforced concrete: an overview after 30 years of development. *Cement Concrete Comp.* **19(2):**107-122.

[2] Maalej, M. and Li, V.C., 1995. Introduction of strain-hardening engineered cementitious composites in design of reinforced concrete flexural members for improved durability. ACI *Struct. J.* **92(2):** 167-176.

[3] Nam, Y.J., Hwang, Y.K., Park, J.W. and Lim, Y.M., 2018. Feasibility study to control fiber distribution for enhancement of composite properties via three-dimensional printing. *Mech. Adv. Mater. Struct.:* 1-5.

[4] Rosewitz, J.A., Choshali, H.A. and Rahbar, N., 2019. Bioinspired design of architected cement-polymer composites. *Cement Concrete Comp.* **96**: 252-265.

[5] Xu, Y., and Šavija, B., 2019. Development of Strain Hardening Cementitious Composite (SHCC) reinforced with 3D printed polymeric reinforcement: mechanical properties. *Compos. Part B-Eng.* Under review.

[6] Xu, Y., Zhang, H., Šavija, B., Figueiredo, S.C. and Schlangen, E., 2019. Deformation and fracture of 3D printed disordered lattice materials: Experiments and modeling. *Mater. Design*. **162***:* 143-153.

[7] Šavija, B., Luković, M., Kotteman, G.M., Figuieredo, S.C., de Mendoça Filho, F.F. and Schlangen, E., 2017. Development of ductile cementitious composites incorporating microencapsulated phase change materials. *International Journal of Advances in Engineering Sciences and Applied Mathematics.* **9(3):** 169-180.

[8] Kanda, T. and Li, V.C., 1999. New micromechanics design theory for pseudostrain hardening cementitious composite. *J. Eng. Mech.* **125(4):** 373-381.